POSSIBLE CURES FOR ELECTRON CLOUD PROBLEMS*

R. J. Macek†
LANL, Los Alamos, NM 87545, USA

Abstract

This paper reviews and evaluates a number of methods and approaches that have been considered and/or explored at the Los Alamos PSR for mitigating the e-cloud problems. The two main approaches are (1) methods to suppress the e-cloud generation and (2) direct methods (such as damping the e-p instability) to control the adverse impact of the e-cloud on accelerator performance. In the first category, we have explored (a) suppression of the primary or "seed" electrons (reduction of losses, improved vacuum, control of the "convoy" electrons at the stripper foil, clearing fields, and suppression of secondary emission at the stripper foil), (b) reduction of electron amplification by beam-induced multipacting (TiN coatings, beam scrubbing, weak solenoids, and shaping the beam pulse), and (c) reduction of electrons that survive the gap (clearing electrodes, and reduction of beam leaking into the gap). While many of these measures suppress multipactor electrons, it is not yet demonstrated that this will cure the e-p instability at PSR. In the second category, we have had success in controlling the e-p instability by various forms of Landau damping (increasing the momentum spread by a variety of methods, multiples, skew quads and inductive inserts) and in controlling the impact on diagnostics by use of bias fields.

1 INTRODUCTION

The characteristics and impact of the electron cloud on accelerator performance can include two-stream instabilities (e.g. at the Los Alamos PSR), vacuum degradation, interference with beam diagnostics, and heat load on superconducting components in the case of LHC. Three of these, the e-p instability, vacuum pressure increases and interference with certain beam diagnostics have been observed at PSR. Most serious for PSR is the two-stream e-p instability, which was first observed at PSR late in 1985, but was not identified as such until the early 1990's [1].

At PSR the search for and development of means to mitigate the e-p instability went on in parallel with work to understand the instability and sources of electrons at a more fundamental level. The two main approaches to cures were (1) methods to suppress the e-cloud generation and (2) direct methods (such as damping the e-p instability) to control the adverse impact of the e-cloud on accelerator performance. To date, the direct methods have been more effective than most of the measures to suppress the e-cloud formation. We surmise that this is a result of suppressing electrons over just a small fraction of the ring circumference.

* Work conducted by the Los Alamos National Laboratory, which is operated by the University of California for the United States Department of Energy under contract W-7405-ENG-36.
†macek@lanl.gov

2 THE E-CLOUD IN PSR

A short summary of the present picture of the electron cloud for stable beams in PSR will aid in interpreting the results of tests of potential cures, which will be described later. We now know that electrons generated by trailing edge multipactor make up much of the electron flux ("prompt" electron signal in Figure 1) striking the wall at the end of the each passage of the bunch [2], [3]. However, electrons captured by the beam pulse from the cold (few eV) electron cloud surviving the beam-free gap between successive passages of the beam bunch ("swept" electron signal in Figure 1) are the main component in the beam neutralization averaged over the beam pulse and thus are the ones that can drive the instability. They also contribute to the "prompt" signal when they are released at the end of the beam on each turn.

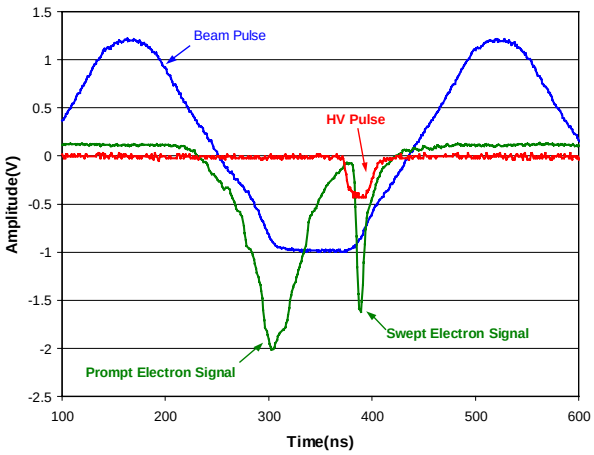

Figure 1. Signals from the electron-sweeping detector in PSR are shown in proper time relationship to the beam pulse. The "prompt" signal comes at the end of the beam pulse and the "swept" electron signal reaches the collector a few ns after the HV pulse is applied to the sweeping electrode [4]. From the swept electron signal timed at the end of the gap one obtains an average neutralization of 1-2% at the location of this detector (section 4 of PSR), which is approximately the value needed to explain the observed instability threshold curves.

The prompt electron intensity depends upon several factors including beam intensity, beam pulse shape, secondary emission yield (SEY) at the vacuum chamber surfaces, the beam losses, vacuum pressure, to name a few. Of special note is the very strong dependence on

beam intensity (stored charge in the ring) as shown in Figure 2 where both the prompt electron signal amplitude and the electrons swept out of the chamber at the end of the gap are plotted as a function of beam intensity. Features to note are the strong dependence on intensity (to approximately the 10^{th} power for the prompt and about the 7^{th} power for the electrons surviving the gap) and the saturation of the swept electron signal above ~5.5 μC/pulse. The saturation of electrons surviving the gap can be qualitatively understood as due to space charge of the electron cloud in the beam-free gap after the bunch.

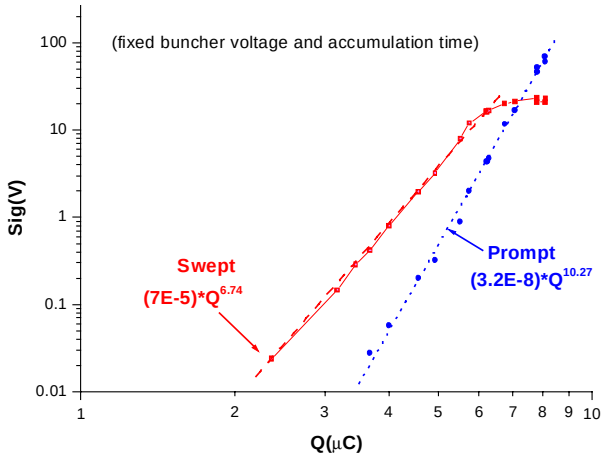

Figure 2. Prompt electron and "swept" electron (swept out of pipe at the end of the gap) signal amplitudes are plotted as a function of stored beam intensity. All other beam parameters were fixed including buncher voltage and accumulation time.

With the electron sweeper we have measured the electron survival as a function of time after the end of the beam pulse. Results are plotted in Figure 3.

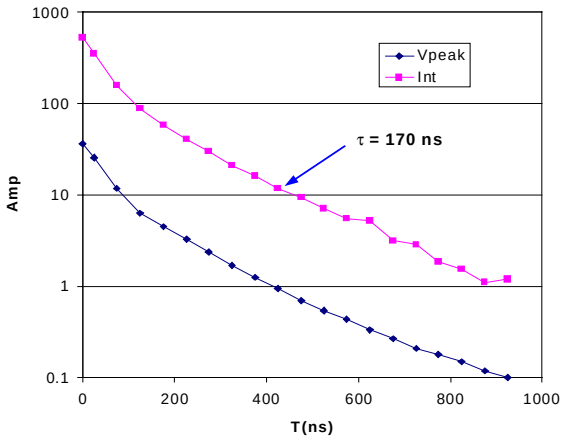

Figure 3. Electron survival plotted as a function of time after the end of the beam pulse. The origin is the end of the beam pulse. The blue diamonds are the peak amplitude (V) of the swept electron pulse while the magenta squares are the integral of the swept pulse (nVs).

An interesting feature of Figure 3 is the long exponential tail indicating that the low energy electrons in the gap can linger for quite some time. It is expected that the average electron in the gap would have an energy near the peak of the secondary emission spectra, which is around 2-5 eV. The exponential behavior in Figure 3 would result from repeated, nearly elastic collisions with the wall in a process having a relatively constant reflectivity, δ, (or, more precisely, secondary emission yield). The electron intensity as a function of time would be proportional to δ^n, where n is the number of collisions with the wall in time t and equal to t/T (T = $d\sqrt{(m_e/2E)}$ is the transit time across the pipe of diameter d). Thus, the exponential time constant for the decaying expeontential is $-T/\ln(\delta)$ and the time constant of Figure 3 implies $\delta \approx 0.5$ for electrons of 2-5 eV. This surprisingly high value of δ is reasonably consistent with recent measurements at CERN [5] for 4 eV electrons on copper. The high "reflectivity" explains the slow decay of electrons in a beam free region and survival of sufficient electrons in the gap to produce the neutralization (1-2%) needed to cause the e-p instability at PSR.

At a routine operating beam intensity of 4-5 μC/pulse, copious electron signals have been observed in PSR where ever electron diagnostics were placed including three different straight sections representing low loss and high beam loss regions and just down stream of the stripper foil. Strong electron signals were also observed on biased collection plates in both quadrupole and dipole magnets. The signal levels are much higher than can be explained by residual gas ionization and are presumed to arise from the same amplification processes (primarily trailing edge multipactor) found in straight sections.

3 CONTROL BY SUPPRESSION OF PRIMARY ELECTRONS

Reduction of the electron cloud by suppression of the primary or "seed" electrons, which are then amplified by beam-induced multipactor, is a potential remedy. At PSR the primary electrons include:

a) Electrons from beam losses where the protons hit the wall at a grazing angle and can produce as many as 100 secondary electrons per incident proton,
b) Electrons stripped from the injected H^- (two 430 keV "convoy" electrons per injected proton plus the secondary electrons from these striking an absorber),
c) Secondary electrons from foil hits by the stored beam,
d) Thermionic emission from the stripper foil, which is heated by the foil hits from the stored beam, and
e) Electrons from residual gas ionization by the beam and the multipacting electrons.

A variety of methods to suppress or control these sources and results of tests are described below.

3.1 Reduction of beam losses and better vacuum

The prompt electron flux striking the walls in a straight section has been measured as a function of local vacuum pressure and local beam losses using a special electron detector, the retarding field analyzer (RFA) developed at

ANL [6]). It has been augmented with fast electronics to provide time resolved signals similar to the prompt signal in Figure 1 [3]. Plots showing the increase in electron signal with increasing vacuum pressure and local beam losses are presented in Figures 4 and 5.

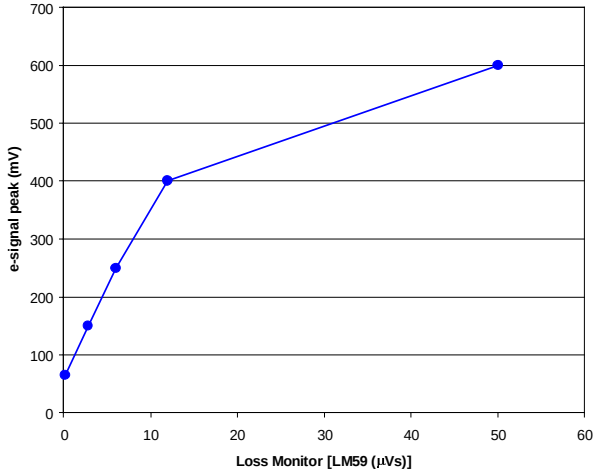

Figure 4. Prompt electron signal as a function of local losses, which were varied by use of a local closed orbit bump. All other beam parameters were held fixed. A local loss monitor placed on the wall opposite the first downstream dipole monitored beam losses. Particles produced at ~ 20° from losses in the first quadrupole just upstream of the electron detector reach the loss monitor.

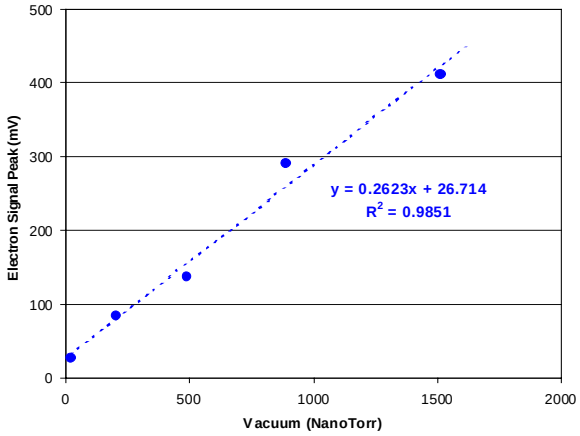

Figure 5. Prompt electron signal amplitude plotted as a function of local vacuum pressure. All other beam parameters were held fixed.

Despite the fact that the prompt electron signals vary with beam losses and residual gas pressure, global increases in losses (factors of 2-3) or vacuum pressure (more than a factor of 100) have had no effect on the instability threshold intensity curves. This long-standing puzzle can be resolved by noting the saturation of the electrons surviving the gap. These are the electrons most likely to drive the instability since they oscillate against the protons during the entire passage of the beam pulse. Thus, increases in losses or vacuum pressure will not increase the electrons driving the instability. In fact measurements of the electrons surviving the gap show absolutely no change when local losses were varied by factors of 2 to 3.

The direct H- injection upgrade of PSR [7] completed in 1998 lowered the beam losses by about a factor of 3 but did not result in an improvement in the instability threshold. In fact, it was worse as seen in the instability threshold intensity curves of Figure 6. However, after several weeks of operation at 100 μA @ 20 Hz the threshold curve returned to the historical value. This is another example of the "conditioning" effect (presumably from electron bombardment by the prompt electrons) seen on other occasions after coming back from a long shutdown where the ring was up to air for months.

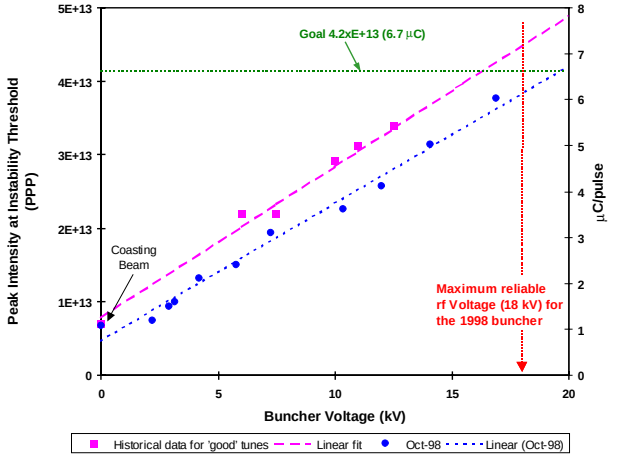

Figure 6. Instability threshold intensity plotted as a function of RF Buncher voltage. The square points are historical data for well-tuned production beams prior to the upgrade and the round points were those taken in October of 1998 during commissioning of the upgrade.

Reduction of losses and improved vacuum will reduce the prompt electron signal approximately linearly in these variables but the data in Figure 2 suggests that it could take an order of magnitude or more reduction in losses and or vacuum pressure to bring the electrons surviving the gap out of saturation and start to improve the instability threshold. Either of these options would require a major rebuild of PSR and are not practical. However, more modest improvements in combination with other measures described later could help mitigate the instability. In addition, any improvement in vacuum or reduction of losses would reduce the prompt electrons striking the wall and thus would help reduce the interference with diagnostics and reduce the vacuum pressure excursions.

3.2 Control of electrons from the stripper foil

The region of the stripper foil hosts several copious but highly localized sources of primary electrons, which were identified at the beginning of this section. Rough analytical estimates of the longitudinal motion of electrons for a typical bunched beam in PSR indicate that most will move less than 0.2 meter depending upon where they were born along the bunch. Thus the cloud density in

this region is expected to be significantly higher than elsewhere.

Since 1998 the stripper foil at PSR has been located in the fringe field of a dipole which deflects the convoy electrons onto a copper absorber ~0.15 meter downstream of the foil. These can make secondaries, which can be amplified by the trailing edge multipactor. It would be better to transport the convoy electrons to an absorber, which can be screened and biased to suppress secondaries as was done in the test described in the next section.

More efficient injection painting, which would reduce foil hits, would reduce the resulting secondary emission and heating of the foil. This was done in the direct H^- injection upgrade of 1998 where the foil hits for a given accumulation time were reduced by nearly a factor of 10. However, the increase in beam current to 100 μA required a 25% longer accumulation time, which meant that the total foil hits were reduced by a smaller factor of ~6.

Thermionic emission is a very strong function of temperature and can be a problem at the higher peak intensities. Biasing the foil with sufficient voltage to overcome the field from the beam can keep both thermionic emission and secondary emission electrons from leaving the vicinity of the foil. This was also tried in a test to be described in the next section.

3.3 Test of electron clearing devices in PSR

Clearing fields, which are strong enough to overcome the field of the beam, can be used to collect electrons from a variety of sources (e.g. beam losses, ionization, and beam losses) before they can multipactor or be captured by the beam. These were tried at PSR in conjunction with various means of controlling electrons in the vicinity of the stripper foil prior to the 1998 injection upgrade [8]. The layout of electron clearing devices in the injection section is shown in Figure 7.

The stripper foil was biased at up to 10 kV to suppress secondary and thermionic emission. The 430 keV convoy electrons and energetic knock-on electrons were deflected to a biased Faraday cup, which was behind a screen that could also be biased separately. The bias fields were configured to suppress secondaries. In addition, the drift spaces before and after the stripper foil were filled with clearing electrodes that could be biased to ± 20 kV respectively. These could be used in conjunction with DC clearing fields applied to the extraction kicker plates in sections 7 and 8, the diagnostic kicker plates in section 3 and to the striplines of three freestanding BPMs in other drift spaces.

When all of the injection devices were energized there was no reproducible effect on the instability threshold. When the other clearing fields were energized as well, there was perhaps a 10-15% increase in the instability threshold consistent with clearing 15% of the circumference of the ring. These results indicate that the injection section is not the main cause of the e-p instability and support the hypothesis that a significant electron cloud is present everywhere in the ring.

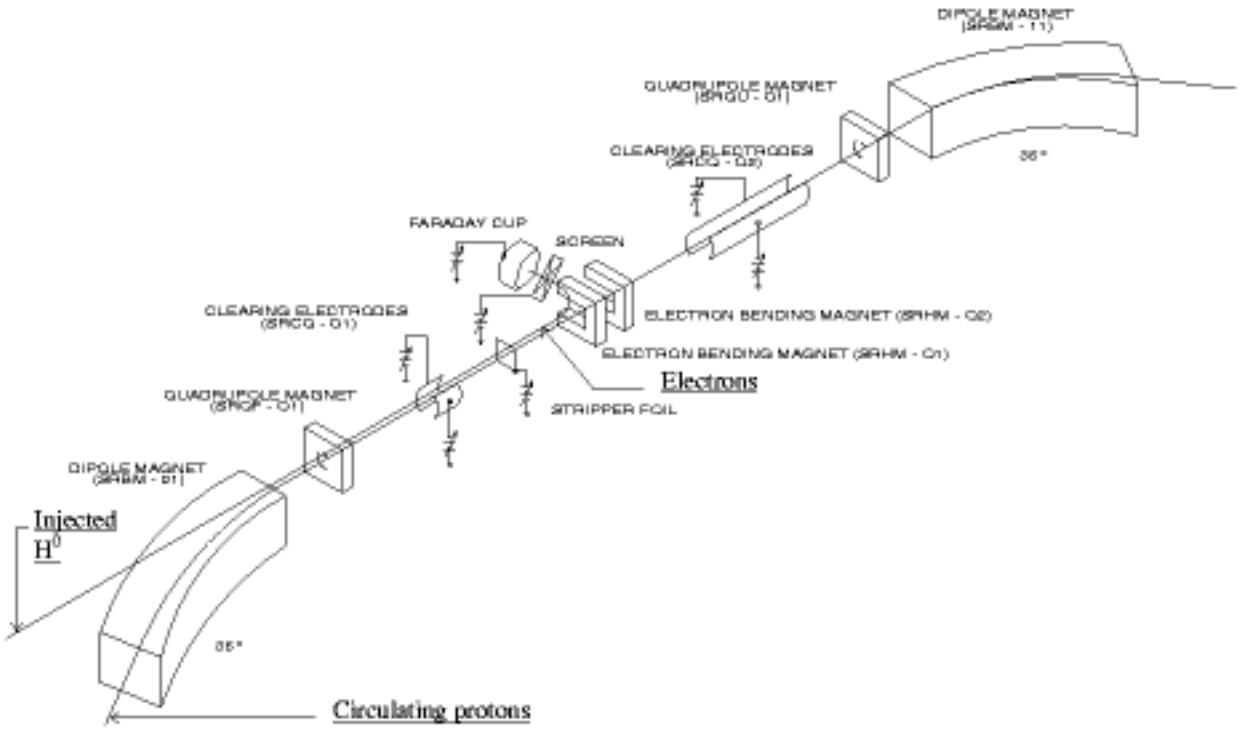

Figure 7 Layout of electron clearing devices in the injection section prior to the 1998 upgrade to direct H^- injection.

4 METHODS TO REDUCE MULTIPACTOR GAIN

Amplification by trailing edge multipactor can have a high gain, which is a strong function of secondary emission yield, but also depends strongly on beam intensity and pulse shape. Some of these features can be manipulated to reduce the multipactor gain and hence the densities of the electron cloud. At PSR we have investigated the effect of vacuum chamber coatings, beam scrubbing, weak solenoids and pulse shape for their efficacy in reducing the multipactor gain. The results of these studies are described in the following subsections.

4.1 Vacuum chamber coatings

A number of different coatings and surface treatments, TiN, C, Cr_2O_3, and TiZrV non-evaporable getter coatings, are known to influence the secondary electron yield (SEY) from electrons with energies below a few keV impinging on the surface. TiN was used to coat the aluminum chambers of the low energy ring (LER) at PEP II to suppress secondary emission. In a test of TiN at PSR (1999), a 3-meter test section of 304 stainless steel vacuum chamber was coated at SLAC using the same process as used for the LER. An identical section, which was not coated, was used for a comparison. The electron signals from the RFA in the center of the two test chambers subjected to an 8 μC/pulse beam are shown in Figure 8.

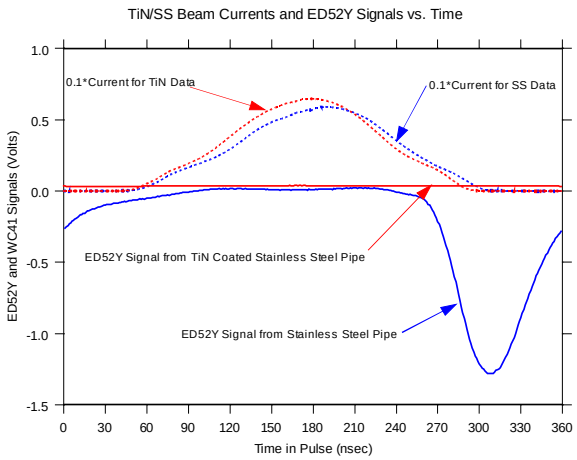

Figure 8. Electron signal from an RFA (designated as ED52Y) in the center of a 3-meter stainless steel test section (solid blue curve) compared with the much reduced (more a factor of 100) electron signal from an identical TiN coated stainless steel section (solid red curve). For reference, the corresponding beam currents are shown (dotted curves).

TiN coating was clearly effective in the reducing the prompt electron signal by a factor of 100 or more. For unstable beams, the RFA electronics were saturated in the uncoated chamber while in the coated chamber a small electron signal was observed which indicated that the detector was still working. How effective the TiN coating is in reducing the electrons surviving the gap or in improving the instability threshold remains to be tested. A definitive test would require coating a large fraction of the ring including the dipoles, which would be expensive and require a long shutdown and, therefore, unlikely to take place. However, a test using a TiN coated electron-sweeping detector in a TiN coated straight section is planned. It would measure the reduction in electrons surviving the gap. A strong reduction in these would be very encouraging for TiN coatings as a cure for the e-p instability.

4.2 Beam scrubbing

Electron bombardment is known to reduce the SEY for some technical surfaces used in accelerators. A "conditioning effect" with respect to the instability threshold curves has been observed at PSR on three occasions after a long shutdown where much of the ring was up to air for maintenance or upgrade (e.g. see the discussion in section 3.1 pertaining to Figure 6). It is presumably due to continued bombardment by the multipacting electrons, which are present even for stable beams. A more systematic study was conducted in 2000 after 4-month shutdown. Results are shown in the sequence of instability threshold curves plotted in Figure 9 below.

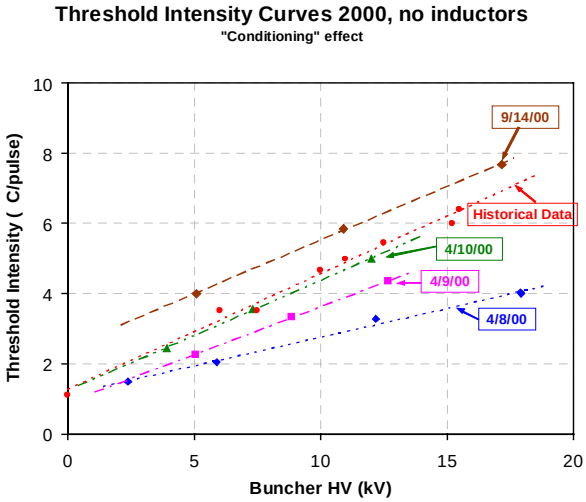

Figure 9. Instability threshold curves at various times after startup in 2000 show a "conditioning" effect.

The lowest curve in Figure 9 was taken on 4/8/00 two days after startup and shows a threshold intensity of only 4 μC/pulse at 18 kV, which is the maximum voltage that can be obtained from the RF buncher. The situation improved a day later after operating for a day at 4-5 μC/pulse. After two days of conditioning the curve about the same as the historical curve. The last curve taken 9/14/00 was obtained after about 6 weeks of routine operation at ~100 μA @ 20 Hz or 5 μC/pulse and shows a factor of two improvement in the threshold intensity at each buncher voltage compared with the lowest curve of 4/8/00.

If the conditioning effect is due to a gradual reduction in SEY then it should also reduce the prompt electrons

signal for a given beam intensity. Experimentally, it tended to diminish over course of time but because the signal is very sensitive to a number of variables, especially peak intensity, a number of corrections are needed to normalize to a given intensity. Such a detailed analysis has yet to be implemented.

4.3 Weak solenoids

Weak solenoids can reduce multipactor gain by turning back low energy electrons leaving the wall and preventing them from reaching the wall with enough energy to make more than one secondary electrons. A 0.5 meter solenoid with an RFA in the center (see Figure 10) was used for a test of the effect on prompt electrons in PSR with results which are shown in Figure 11 and 12.

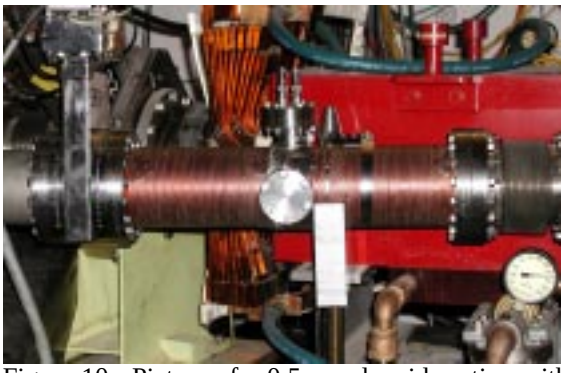

Figure 10. Picture of a 0.5 m solenoid section with an RFA in the center (installed in section 9 of PSR).

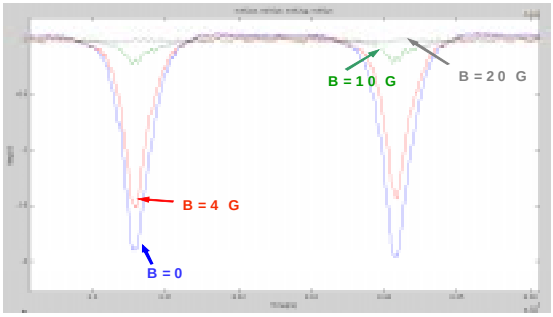

Figure 11. Prompt electron signals from the test solenoid for 3 values of the magnetic field (in Gauss). Signals are shown for two turns.

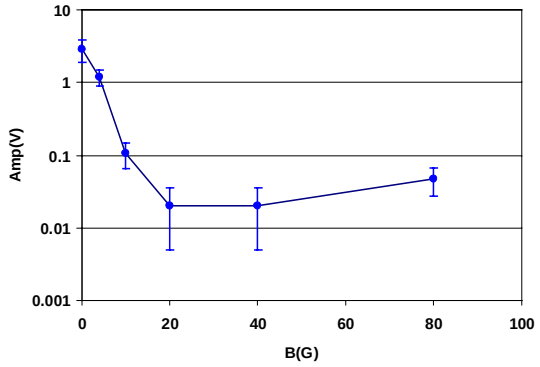

Figure 12. Curve showing the prompt electron signal from the test solenoid plotted as a function of magnetic field B (in Gauss) in the solenoid.

As can be seen in Figures 11, and 12, weak solenoid fields are effective in suppressing the prompt electrons by a factor of about 50 even in this relatively short solenoid where some electrons from the nearby straight sections (with no field) might leak in from the ends. However these measurements do not give any indication as to how many electrons remain in the pipe during the gap. Because of the solenoid field, it would difficult to use an electron sweeper to measure electrons remaining in the pipe unless the voltage could be raised to several kV. Despite the uncertainty on electrons surviving the gap, solenoids show promise for suppressing the electron cloud in a long bunch ring such as PSR. There are plans to cover about 10% of the ring circumference with solenoids as a test (in the coming run cycle) of their effect on the instability threshold in conjunction with TiN coatings in another 5% of the circumference.

4.4 Tailoring the pulse shape

Pulse shape is another parameter that has a significant influence on the prompt electron signal amplitude. This is not surprising for electrons from trailing edge multipactor, which are sensitive to the derivative of longitudinal profile of the beam pulse. Pulse shape, to the extent that it can be manipulated, becomes another variable in the overall minimization of the multipactor gain. The effect of pulse shape was studied at PSR by adjusting the rf buncher phase which produced subtle changes in shape of the trailing edge as shown in Figure 13. The prompt electron signals for these shape variations are shown in Figure 13.

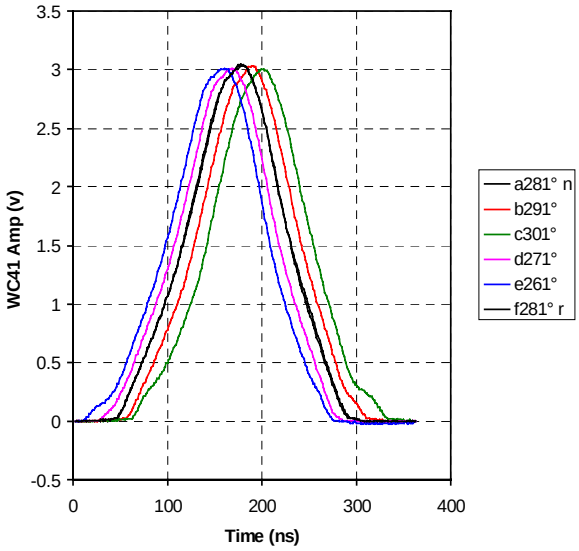

Figure 13. Effect of rf buncher phase variations on the beam pulse shape as measured with a wall current monitor (WC41).

In Figure 13 the nominal phase was 281° (trace a and a repeated run, trace f). Departures from nominal in either direction produced a shoulder on one side of the pulse or the other depending on whether the phase was increased or decreased. Increasing the phase to 301° (trace c301°) produced the largest shoulder on the trailing edge, a

situation that produced the greatest change in the prompt electron signal amplitude in Figure 14 (trace c301°).

The lowest electron amplitude is trace d271° (close to the nominal setting of 281°), which is the setting that produced the smoothest trailing edge in Figure 13 A complete study of the optimal shape has not been carried out. This is perhaps best done by first studying the effect of various shapes in simulations then checking it experimentally. We have presented just one class of pulse shape variations using the buncher phase and it indicates that one should operate without shoulders on the trailing edge, which is achieved by injecting in the center of the rf bucket. This indication is also consistent with earlier observations that the instability threshold is maximized by centering the beam in the rf bucket [9].

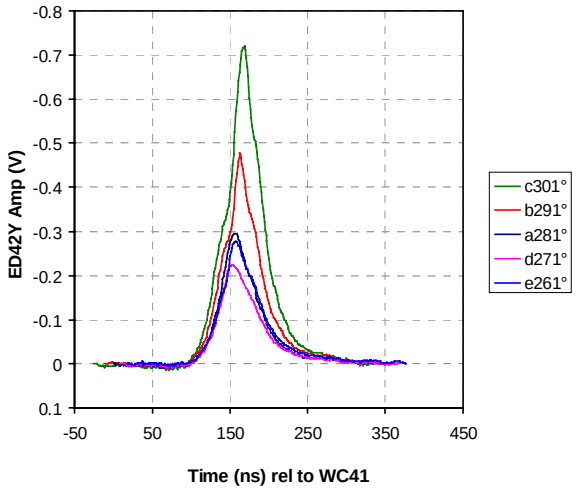

Figure 14. Effect of rf buncher phase variations on the prompt electron signal for detector ED42Y. The trace labels in the legend are keyed to the same ones as in Figure 13.

5 REDUCTION OF ELECTRONS SURVIVING THE GAP

Since the most damaging component of the electron cloud for the e-p instability is the electrons that survive the gap, reducing these would be a most effective cure.

5.1 Reduction of beam in the gap

It was once thought that beam leaking into the gap and trapping electrons was a key ingredient in the cause of the e-p instability [1]. In fact, adding beam in the gap did lower the instability threshold in experiments at PSR. Beam was added to the gap by inhibiting the chopper and injecting a number of unchopped turns in the ring. The buncher voltage at instability threshold for two fixed intensities of different bunch widths is plotted as a function of added beam in the gap in Figure 15. Adding beam to the gap increases the buncher voltage required to reach the instability threshold for fixed intensity beam. This is equivalent to lowering the threshold intensity for a fixed buncher voltage. This data shows that beam in the gap at the few percent level can affect the instability. Therefore, it is important to keep the gap quite free of beam (< 0.1%). It can be controlled by the rf system and the use of inductive inserts, which are described later in section 6.4. At PSR today, beam in the gap is typically <0.05% and is therefore not a significant factor in causing the instability.

In recent experiments with added beam in the gap both the prompt and the swept electrons increased. One expects the electrons surviving the gap to increase by the amount of beam added to the gap so as to neutralize the added protons. This was approximately what was observed.

With added beam in the gap the additional electrons surviving the gap will also be captured by the next beam pulse and then be released at the end of the pulse to contribute additional electrons to the prompt electron signal, as was also observed in these experiments. It would be informative to use an electron cloud simulation program, such as the LBNL simulation code POSINST to simulate the effect of beam in the gap for comparison with the experimental results. This would provide a better indication of the expected effects of beam in the gap than the more qualitative picture outlined above.

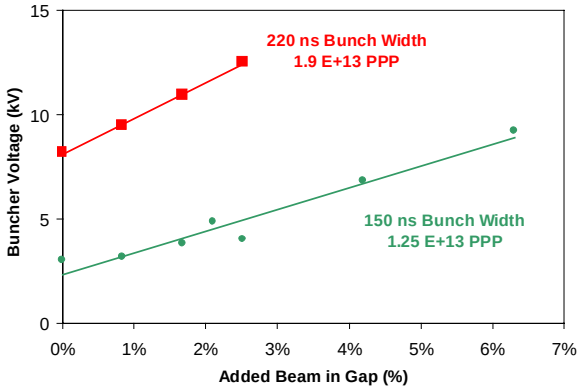

Figure 15. This graph shows the effect of added beam in the gap. The instability threshold buncher voltage is plotted as a function of added beam in the gap for two different beam intensities.

5.2 Vacuum chamber coatings and beam scrubbing

From recent measurements at CERN [5] it is now known that for Cu surfaces at least that the SEY for very low energy electrons is reduced with electron bombardment. This means that beam scrubbing or beam conditioning should reduce electrons the decay time for electrons surviving the gap, hence their number as well. This may be the cause of the conditioning effect on the instability threshold curves at PSR.

Will TiN or other coatings that reduce the SEY at the peak of the energy dependence have the same effect on low energy electrons i.e., reduce the decay time for electrons in the gap? This intriguing possibility will be checked at PSR in the near future in measurements using a TiN coated electron-sweeping detector placed in a TiN coated straight section.

6 METHODS TO DAMP THE E-P INSTABILITY

Another approach to mitigating the e-p instability is to invoke various methods of damping the instability. A number of methods have been tested at PSR in the past few years and are discussed in the subsections that follow.

6.1 Increased rf buncher voltage

Increased rf buncher voltage was the first method used to control the instability. It was observed early on that the instability threshold intensity was rather linear in rf buncher voltage as shown in Figure 14 (also see Figure 5 and 8). The linear behavior implies that the instability threshold intensity varies as the square of the momentum spread and can be understood in the coasting beam model with Landau damping if the fractional neutralization is constant [10].

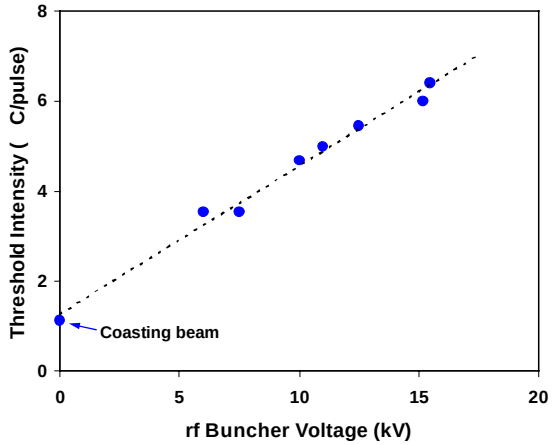

Figure 16. Instability threshold intensity as a function of rf buncher voltage. These are historical data for well-tuned production beams prior to the 1998 injection upgrade.

Because the rf buncher voltage has been our most effective control for the instability, the buncher was upgraded in 1998 to raise the reliable operating voltage from 12 kV to 18 kV in order to permit going to higher intensity. There is, however, a downside to higher momentum spread and that is increased beam losses in the ring at the higher rf voltages.

6.2 Landau damping with multipoles

Landau damping with magnetic multipoles (sextupoles and octupoles) has also been found to be effective. An example is the effect of an octupole field on the rf buncher threshold voltage for a fixed beam intensity of 5 μC/pulse as shown in Figure 17. The octupole significantly reduces the buncher voltage at the instability threshold. This is equivalent to increasing the threshold beam intensity for a fixed buncher voltage. The graph also shows the down side of using multipoles i.e., the beam losses increase as a nonlinear function of octupole excitation.

The effect of sextupoles was similar but will not be shown here. However, Figure 19 does show the beneficial effect of sextupoles to augment the benefits of inductive inserts. There is also evidence that the main effect of sextupoles on the instability is not through the change in chromaticity (effect was the same regardless of polarity) but to introduce transverse coupling. If the closed orbit is offset in a sextupole this introduces a skew quadrupole field component and, as will be shown in the next subsection, a skew quad excitation produces coupled Landau damping which is also effective in damping the instability.

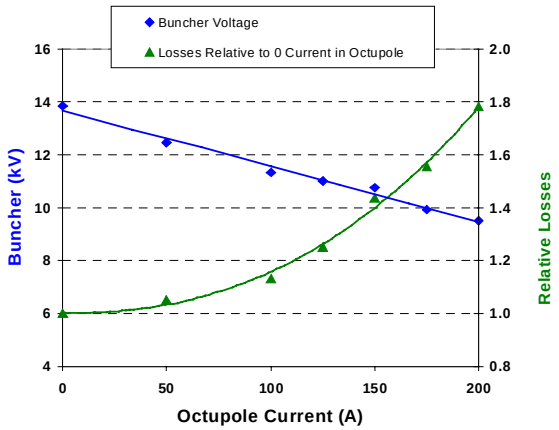

Figure 17. Instability threshold voltage (blue diamonds) plotted as a function of octupole current. Also shown are relative beam losses (green triangles) as a function of the octupole current.

6.3 Coupled Landau damping

Coupled Landau damping [11] has been tested and found effective at PSR. In these tests the operating point was tuned to be on the coupling resonance Qx-Qy = 1 and a single skew quad was weakly excited. The results are shown in Figure 18.

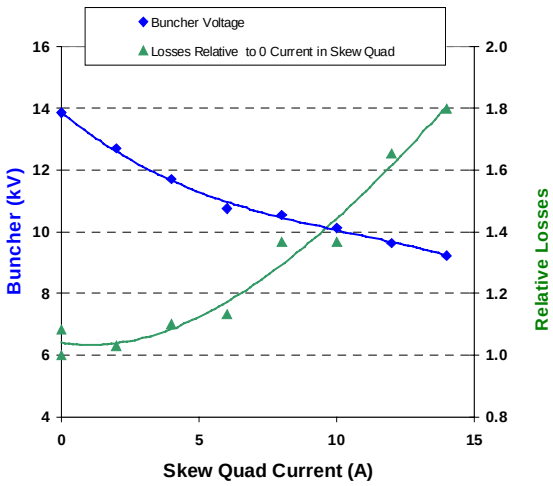

Figure 18. Instability threshold voltage (blue diamonds) plotted as a function of skew quad current. Also shown are relative beam losses (green triangles) as a function of the skew quad current.

6.4 Inductive inserts

Inductive inserts were tried in a collaborative effort with FNAL [12], [13] as part of the Short Pulse Spallation Source Enhancement Project (SPSS) at PSR. The original motivation was that passive compensation of longitudinal space charge force by the ferrite inserts would prevent beam leaking into the gap and hence would improve the instability threshold. Indeed, with the inserts the gap appears flatter and with a sharper transition between the beam and the gap. The inserts are equivalent to more rf with the harmonics which compensate the longitudinal space voltage that is proportional to the derivative the line density of the beam. Inserts would also increase the momentum spread and cause additional Landau damping by removal of the potential well distortion that depresses bucket height.

The effect of the inductive inserts on the instability threshold curves is shown in Figure 19. The instability threshold intensity improves by ~35% with inductive inserts alone. The improvement is the amount expected from the increased momentum spread of the equivalent rf. When the sextupoles were excited in the presence of the ferrite inserts, additional improvement in the threshold intensity was obtained suggesting that the improvements are approximately additive.

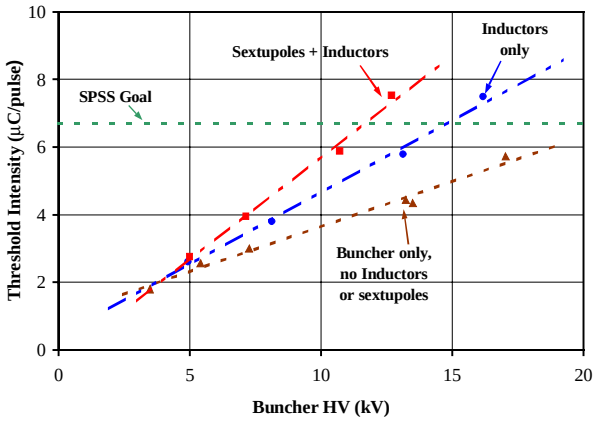

Figure 19. Graph showing the effect of inductive inserts and sextupoles on threshold intensity curves. The inductance of the inserts was 11 μH, which is the amount needed for full compensation of longitudinal space charge at PSR.

With the ferrite inserts it was also possible to increase the bunch width without affecting the instability. This helped reduce the accumulation time needed for a fixed intensity and resulted in useful savings of linac duty factor and power.

7 CONCLUSIONS

From experiment and simulations it is known that trailing edge multipactor at PSR produces a large amplification of primary electrons and, as such, is responsible for the vacuum degradation and interference with some diagnostics. Electrons, which survive the gap to be captured by the subsequent beam pulse, are the main component to average beam neutralization and are the ones expected to drive the e-p instability.

Suppression of the electron cloud by reduction of the primary or "seed" electrons (from beam losses, residual gas, and stripper foil processes) reduces the prompt electrons from the multipactor process in PSR but have not been sufficient to reduce the electrons surviving the gap. This is likely due to the saturation (at higher beam intensities) of the electrons in the gap. While presently available means to suppress the primary electrons are not sufficient to cure the instability they might be effective in combination with other methods.

TiN coatings and weak solenoids do greatly suppress the multipactor gain but it has not yet been demonstrated experimentally that they will greatly reduce the electrons surviving the gap. A test planned at PSR for the 2002 run cycle will measure the effect of TiN coatings on the electrons surviving the gap.

Beam scrubbing or conditioning is effective in reducing the prompt electron signal and in raising the instability threshold by a factor of two at PSR. Presumably, this is due to a reduction of the SEY by electron bombardment.

Bias fields to repel electrons have reduced the spurious signals on certain diagnostics affected by the electron cloud. It is anticipated that coatings such as TiN to suppress multipactor will also help these diagnostics.

Landau damping by increased rf voltage, transverse coupling, multipoles and inductive inserts have significantly raised the instability threshold but with some increase in losses. These measures along with some condition beam conditioning have allowed us to raise the stable peak intensity at PSR to 10 μC/pulse (6.3×10^{13} protons per pulse) of stored charge, which is a factor of two above the design goal of the 1998 upgrade and 50% above the SPSS project design goal.

8 ACKNOWLEDGEMENTS

Many people contributed in the past several years to the work reviewed and discussed here. I gratefully acknowledge the innumerable contributions from the other members of the PSR development team at LANL including Andrew Browman, Daniel Fitzgerald, Mike Plum, Mike Borden, Frank Merrill, Thomas Spickermann and Rod McCrady. Robert Kustom (ANL) introduced us to the RFA provided by Kathy Harkay and Richard Rosenberg and gave us much encouragement and support to resolve the instability, which he deemed a significant technical risk for the SNS project. Jim Griffin, Bill Ng and David Wildman at FNAL were collaborators on the effort to test inductive inserts. Slava Danilov, Sasha Alexandrov and David Olsen at SNS were collaborators on the test of TiN coatings. Dan Wright of SLAC coated the chambers with TiN for these tests. I also acknowledge many useful discussions with the PSR instability collaboration at LANL, LNBL, ANL, BNL, and PPPL including Tai-Sen Wang, Paul Channel, Miguel Furman, Mauro Pivi, Glen Lambertson, Kathy Harkay, Mike Blaskiewicz, Ron Davidson and Hong Qin.

9 REFERENCES

[1] D. Neuffer et al, “Observations of a Fast Transverse Instability in the PSR”, NIM A 321 (1992), p. 1-12.

[2] R. Macek et al, “New Developments on the e-p Instability at the Los Alamos Proton Storage Ring”, Proceedings of ICANS-XV, 6-9 November 2000, Tsukuba, p 229-239 (March 2001).

[3] R. Macek et al, “Electron Proton Two-Stream Instability at the PSR”, Proceedings of PAC2001, Chicago, June 18-22, 2001, p 688-692, (2001).

[4] A. Browman, private communication and T.S. Wang, et al, “The Static Electric Field of a Curved Electrode in a Beam Pipe”, PSR Technical Note 01-003 (2001). Also see R. Macek PI, LANL LDRD Progress Report, LA-13923, p 134-136, (2001).

[5] N. Hilleret et al, “A Summary of Main Experimental Results Concerning the Secondary Emission of Copper”, CERN LHC Project Report 472, August 2001.

[6] R. Rosenberg and K. Harkay, “A rudimentary electron energy analyzer for accelerator diagnostics”, NIM A 453 (2000) p507-513.

[7] D. Fitzgerald et al, “Commissioning of the Los Alamos PSR Injection Upgrade”, Proceedings of PAC99, March 29-April 2, 1999, New York, p 518-520 (1999).

[8] M. Plum, “Electron Clearing in the Los Alamos Proton Storage Ring”, Proceedings of the 1995 PAC, May 1-5, 1995 Dallas, p 3406-8, (1995).

[9] M. Plum et al, **“**Beam parameters that affect the PSR beam instability”, PSR Tech Note 97-019, (1997).

[10] R. Macek, “PSR Instability”, Buncher II Workshop, LANL, Jan 19, 1999.

[11] E. Metral, “Theory of Coupled Landau Damping", Particle Accelerators, vol. 62(3-4), p. 259, January 1999.

[12] M. A. Plum et al, “Experimental study of passive compensation of space charge at the Los Alamos National Laboratory Proton Storage Ring”, Phys. Rev. ST Accel. Beams 2, 064210 (June 1999).

[13] K.Y. Ng et al, “Recent Experience with Inductive Inserts at PSR”, Proceedings of PAC2001, Chicago June 18-22, 2001, p 704-6, (2001).